A Biophysical Analysis of Neutrophil Force Generation in a Biochemical Environment

By

Christina Andrews

B.S., Brown University, 2017

Thesis

Submitted in partial fulfillment of the requirements for the
Degree of Master of Science in the Department of Biomedical Engineering at Brown University

PROVIDENCE, RHODE ISLAND

MAY 2018

This thesis by Christina Andrews is accepted in its present form
by the Department of Biomedical Engineering as satisfying the
thesis requirements for the degree of Master of Science

Date _____ _____
(Signature)

_____
(Christian Franck, Ph.D.)
Thesis Advisor

Date _____ _____
(Signature)

_____
(Craig Lefort, Ph.D.)
Committee Member

Date _____ _____
(Signature)

_____
(Jonathan Reichner, Ph.D.)
Committee Member

Date _____ _____
(Signature)

_____
(Ian Wong, Ph.D.)
Committee Member

Approved by the Graduate Council

Date _____ _____
(Signature)

_____
(Print Name)
Dean of the Graduate School

Acknowledgements

Thank you to everyone at Brown who helped me complete my thesis. First and foremost my advisor Dr. Christian Franck, for providing an excellent lab environment to grow intellectually and professionally, and for his mentorship during my time at Brown. Dr. Michael Harman for his tremendous support during my thesis project, his troubleshooting advice, and support to become a better scientist. All Franck Lab members for introducing me to a lab environment four years ago, showing me the ropes since then, and willingness to help and answer all of my questions.

Contents

List of Figures

List of Tables

Chapter 1

Introduction

Neutrophils are a type of polymorphonuclear leukocyte that play a crucial role in the innate immune system. They act as first responders when recruited to an inflammatory site, and their primary role is to protect the body against invading pathogens. The precise recruitment of neutrophils to the site of inflammation is critical to ensure the clearance of the infection [1]. The Franck Lab is focused on establishing a baseline on the relationship between mechanics and cellular mechanisms, with a focus on neutrophil migration and adhesion. This will provide information moving forward to understand what biochemical or mechanical sensing causes the neutrophil to recognize that there is an injury, and then what forces it to migrate to the site of injury.

As the half-life of neutrophils is less than 10 hours, they store all of their cytotoxic molecules in various granules for the extent of their life. The release of these intracellular molecules is a key component in killing bacteria, however over-release can result in tissue injury in the presence of inflammatory conditions, including sepsis and septic shock [15]. Sepsis is a bacterial infection that results in a complex, systemic response that directly impacts the host's innate immune response. In a septic host, neutrophils become over-activated by chemical stimuli and begin to inflict tissue damage, cause organ dysfunction, and even death.

As mechanics play a huge role in neutrophil function, the Franck lab and Reichner lab have collaborated to create the tools that allow us to study these movements. The lab has established a sophisticated traction force microscopy (TFM) technique that is ideal for studying neutrophil motility because it accounts for large material deformation on a personal computer's graphic processing unit (GPU) to produce high resolution, signal-to-noise, high efficiency computations. This innovative approach uses a

fast iterative digital volume correlation (FIDVC) method to study in-plane and out-of-plane neutrophil motility and surface traction stresses.

The novel engineering technology in the Franck lab presents a unique opportunity to collaborate between the study of immunology in the Reichner lab and engineering to further understand the motility of neutrophils. The information that we gain in this study can be utilized to further study the migration of healthy neutrophils compared to damaged neutrophils, such as in the presence of autoimmune disorders. Long term, the Franck lab aims to create an equation of motion and set a baseline for what can be considered healthy human neutrophil activity, such that it can be used to study damaged neutrophils present in a patient with an autoimmune disorders, where motion becomes anomalous and defective.

A significant decrease in the number of neutrophils in the circulating blood stream is directly correlated to severe immunodeficiency in humans. This project aims to better understand the biochemical mechanisms that help regulate neutrophil migration and recruitment to a site of infection, and how the tissue properties help shape the neutrophil response. The clinical motivation behind studying neutrophil migration and adhesion is to aid in the discovery of new therapies for cell-based migration disorders, such as autoimmune diseases or cancer.

The specific aims of this thesis project are as to quantify the change in neutrophil material displacement fields and surface traction stresses as it relates to a two-step activation process on polyacrylamide hydrogels. Also, I will analyze the change in neutrophil material displacement fields and surface traction stresses as it relates to polyacrylamide stiffness and protein coating.

I will achieve the first aim by priming neutrophils with 1 nM fMLP on polyacrylamide hydrogels (E = 1.7 kPa and 8.7 kPa), and use laser scanning confocal microscopy (LSCM) to follow the change in neutrophil characteristics before and after the addition of 200 ng/mL lipopolysaccharide (LPS). I will achieve the second aim by comparing neutrophil response to 50 μg/mL ICAM-1 and 200 μg/mL fibronectin on polyacrylamide hydrogels (E = 1.7 kPa and 8.7 kPa). Human ICAM-1 will be used to mimic

rolling and adhesion to the endothelium after the host detects pathogens at a site of inflammation. Human fibronectin will be used to mimic transmigration through the endothelium and movement towards the site of inflammation.

I aim to understand how neutrophils adapt to different mechanical and biochemical environments to further learn key similarities and differences of neutrophils and their role in inflammation, infection, and autoimmune diseases.

Chapter 2

Background

2.1 Neutrophil Mechanobiology

The mechanical properties of a cell body play a major role in cell motility. As neutrophils are amoeboid, they possess the ability to alter their shape by extending and retracting pseudopods. The migration of all amoeboid cells involves a series of steps that require modulation of receptor-mediated interactions between cells and their environment to aid in adhesion, force generation, and the geometric adaptation of the cell itself to maneuver through biological tissue [2]. Amoeboid-like cells rely on spreading to attach to multiple binding sites and pull forward on 2D surfaces [1]. Neutrophil migration relies on constant contact with the surrounding environment to provide friction in order to produce internal traction forces, which are then converted into directed forward motion [2]. This plays a crucial role in forming the recruitment cascade and understanding neutrophil motility. As neutrophils are present in multiple microenvironments throughout the body, they must be able to adapt to the surrounding chemical and mechanical characteristics. This is key in understanding the neutrophils role in the innate immune response.

Elimination of bacteria relies on the rapid recruitment of neutrophils to the site of infection. In order for neutrophils to reach this location, they must first adhere to the endothelium and then actively migrate into the extracellular matrix (ECM) in response to chemical stimuli [4]. This requires the combined work of selectins, integrins, and chemokines to stimulate the endothelium, and create pathogen-induced adhesion and migration of neutrophils to the site. Selectins promote the first stage in the recruitment cascade of initial rolling and tethering to the endothelium, and integrins promote firm adhesion.

Selectins are a family of glycoprotein surface adhesion molecules, including E-selectin expressed on endothelial cells, L-selectin expressed on leukocytes, and P-selectin expressed on platelets and endothelial cells [3]. L-selectin is constantly expressed on the surface of neutrophils regardless of the presence of chemical stimuli, defining it as a constitutive integrin. E- and P-selectin expression is upregulated on the endothelium after activation by chemokines or other inflammatory mediators, defining it as an induced integrin.

Integrins are a family of transmembrane receptors that facilitate neutrophil-endothelium adhesion. They are classified with an α chain and a common β chain to help define subfamilies. The two key roles of integrins are to act as adhesive proteins and signaling molecules during the inflammation process [7]. The integrins most important to neutrophil adhesion are β-1 and β-2 integrins. Specifically, the β-2 integrins lymphocyte function-associated antigen 1 (LFA-1) and macrophage receptor 1 (Mac-1).

Neutrophils are stimulated by chemokine receptors, which can be induced by the presence of pathogens, and these intracellular signals activate integrins to induce binding to their respective ligands in the extracellular matrix (ECM) [7]. Binding to the ECM involves molecules of the immunoglobulin superfamily that are present on the endothelium, such as intracellular adhesion molecule 1 (ICAM-1) and vascular cell adhesion molecule 1 (VCAM-1) [3]. Table 2.1 below provides a list of adhesion molecules and defines its cellular location [4].

After adhesion, neutrophils require a chemoattractant gradient to aid in extravasating through the endothelium. The chemokines on the endothelium are positively charged molecules that induce conformational changes of the surface-expressed, constitutive integrins on the neutrophil. Additionally, the chemical stimuli triggers induced integrins to relocate to the cell surface and prepare for binding and adhesion. Chemoattractants are chemical stimuli that help direct neutrophils to the site of inflammation, such as the release of the chemokine, lipopolysaccharide (LPS), from a bacterial infection to signal neutrophils to the site [3]. This creates an affinity for the constitutive integrins to

TABLE 2.1: Adhesion molecules involved in neutrophil-endothelial cell interaction, crawling and arrest. Re-created from Brown et. al. [4].

Alternative Name	**Expressed on cell type**
Selectins	
E-selectin	Endothelium
L-selectin	Neutrophils
P-selectin	Endothelium
β1 integrins	
VLA-4	Septic neutrophils
VLA-3	Septic neutrophils
β2 integrins	
LFA-1	Neutrophils
Mac-1	Neutrophils
Ligand for β1 integrins	
VCAM-1	Endothelium, induced by cytokines
Ligand for β2 integrins	
ICAM-1	Endothelium, upregulated by cytokines

bind to their subsequent ligands, such as cell adhesion molecules (CAMs) [1]. The interactions that occur between specific chemokines and leukocytes are the mechanisms in which the innate immune response recruits specific subsets of leukocytes to specific areas of infection. Integrin activation and binding plays a crucial role in neutrophil adhesion, and the presence of chemical stimuli aids in directing neutrophils through the recruitment cascade to the site of infection [1].

2.2 Neutrophil Recruitment Cascade

The traditional neutrophil recruitment cascade involves tethering to the endothelial cell surface, rolling on the endothelium due to activation by chemical stimuli, crawling to a cell-cell junction, and transmigration to the site of infection.

2.2.1 Tethering

Initial neutrophil recruitment occurs by stimulating the endothelial surface by inflammatory mediators. These chemical stimuli are initially released by leukocytes through

pattern-recognition receptor (PRR)-mediated detection of pathogens, which can increase expression of adhesion molecules [2]. P-selectin and E-selectin are then upregulated on the endothelial cell surface to help maximize neutrophil recruitment. This step helps facilitate contact of free-flowing neutrophils to the chemokine-covered endothelium to help promote activation. Full activation may require two steps; an initial priming step by pro-inflammatory cytokines or contact with the activated endothelium, and then exposure to pathogen-associated molecular patterns (PAMPs), growth factors, or chemoattractants [1]. This two-step process is combined to capture and tether free-flowing neutrophils to the endothelium and rolling along the vessel with the blood stream.

2.2.2 Rolling

The rolling step in the neutrophil recruitment cascade harnesses physical and molecular forces mediated by selectins and their ligands. Neutrophil rolling on the endothelium is severely affected when selectins are blocked because this step helps them connect with inflammatory factors on the endothelium, such as interleukin-8 (IL-8), formyl-methionyl-leucyl-phenylalanine (fMLP), and platelet-activating factor [4]. This connection stimulates the neutrophils to upregulate and increase their avidity of β-2 integrins for the endothelial ligand. This can be seen when LFA-1 and Mac-1 are activated by the endothelium and encouraged to bind to common cell surface molecules like ICAM-1 and ICAM-2 [4].

Neutrophil rolling involves the initial step in which long membrane tethers are formed at the back of the cell, that then 'catapult' to the front of the rolling cell [1]. These tethers are coated in LFA-1, which binds to ICAM-1 and ICAM-2 on the endothelial surface and aids in neutrophil arrest on the endothelium.

2.2.3 Crawling and Arrest

The rolling step of neutrophils helps prepare for extravasation through the endothelium, however this does not always occur at the initial site of arrest on the endothelial

surface. Neutrophils possess the feature to 'probe' their surrounding area to continue scanning for activation by chemical stimuli and an ideal location to transmigrate [1]. This ability allows the cells to elongate and reach out pseudopods, while remaining securely attached to the endothelium. Ideally, neutrophils begin to transmigrate at cell-cell junctions on the endothelial surface, which may require them to actively crawl towards. Specifically, the crawling step requires constant adhesion to the endothelium, mediated by the neutrophil-expressed integrin Mac-1 binding to and releasing from the endothelial cell-expressed ICAM-1 in a forward motion [1]. Figure 2.1 below depicts neutrophil rolling, integrin activation, and arrest on the endothelium in response to a chemical stimuli [4].

The β-1 integrin VLA-4 and β-2 integrin LFA-1 play a key role in integrin-mediated adhesion. This step in the recruitment cascade relies on chemokines to quickly regulate integrin avidity in a cell-specific manner by increasing integrin affinity, meaning that induced integrins within the neutrophil will relocate to the outside of the cell to prepare for adhesion to the endothelium and help regulate cell motility and proliferation [16].

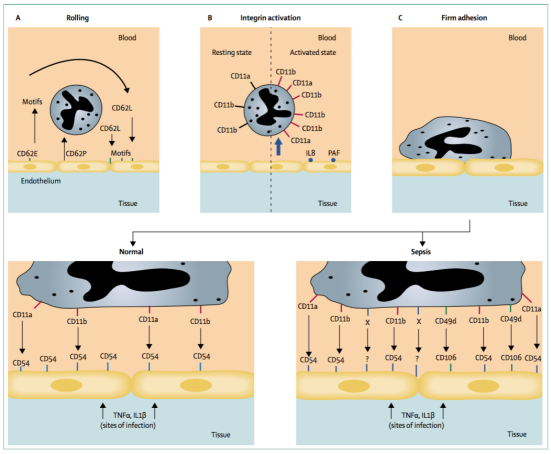

FIGURE 2.1: Neutrophil migration to the site of infection relies on rolling on the endothelium, activation by inflammatory stimuli expressed on the endothelium, and firm adhesion. **A.** L-selectin on the neutrophils and E-selectin and P-selectin on the endothelium activate and induce rolling and tethering to the surface. **B.** There is an increase in inflammatory molecules on the endothelium due to the presence of pathogens, which increases surface expression and avidity of β-2 integrins, LFA-1 and Mac-1, on neutrophils to promote firm adhesion to the endothelium. **C.** In healthy neutrophils, LFA-1 and Mac-1 promote firm adhesion through interaction with ICAM-1, which is upregulated by pro-inflammatory cytokines. In septic neutrophils, the similar process takes place but at an increased amount. Neutrophil adhesion is increased with the help of VLA-4 and VCAM-1 [4]. Figure re-printed from Brown et. al. [4].

2.2.4 Transmigration

In order to migrate towards the site of injury, neutrophils must exit the endothelium through cell-cell junctions. This requires the help of integrins and CAMs: ICAM-1, ICAM-2, and VCAM-1. Endothelial cells develop projections that move up the sides of the neutrophil and extend to the top of the cell to form domes and protect the neutrophil from the shear of the blood stream [1]. Transmigration of neutrophils requires endothelial cells to undergo conformational surface changes and rearrange their focal adhesions to connect to the extracellular matrix (ECM) [1].

In this step, neutrophils follow a chemokine gradient to extravasate through the endothelium. Following extravasation neutrophils must go against this gradient, which

indicates a hierarchy of chemokines. The chemoattractant molecules that are emitted from the site of infection, such as bacteria-derived LPS, overrides the chemotactic signal released from the endothelium to promote transmigration to the site.

2.3 Importance of Studying Sepsis

The innate immune system plays a major role in responding to infection or inflammation in the body, which is regulated by circulating leukocytes that rapidly detect and respond [8]. Neutrophils are known to play a pivotal role in removing bacterial infections, but consistent infections put the patient at high risk of developing sepsis. Sepsis is a severe bacterial infection that has a direct effect on the host's immune response. It has the ability to impair immune function by inducing defects in innate immunity [8]. The criteria in diagnosing sepsis requires an abnormal neutrophil count, which is a key indication of the significant role that neutrophils play in the immune response and the direct negative impact that sepsis plays on the function of these cells [4]. Figure 2.2 below shows a list of symptoms that help clinicians diagnose sepsis by analyzing the function of multiple physiological systems [4].

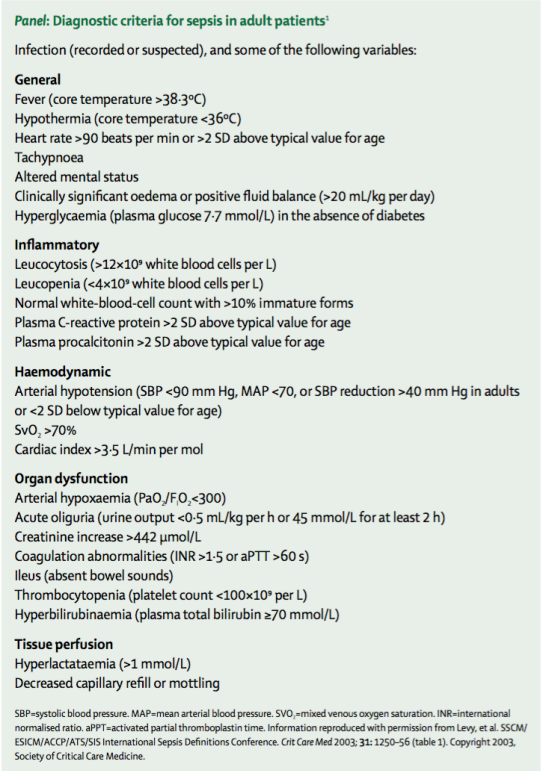

***Panel*: Diagnostic criteria for sepsis in adult patients**[1]

Infection (recorded or suspected), and some of the following variables:

General
Fever (core temperature >38·3°C)
Hypothermia (core temperature <36°C)
Heart rate >90 beats per min or >2 SD above typical value for age
Tachypnoea
Altered mental status
Clinically significant oedema or positive fluid balance (>20 mL/kg per day)
Hyperglycaemia (plasma glucose 7·7 mmol/L) in the absence of diabetes

Inflammatory
Leucocytosis (>12×10⁹ white blood cells per L)
Leucopenia (<4×10⁹ white blood cells per L)
Normal white-blood-cell count with >10% immature forms
Plasma C-reactive protein >2 SD above typical value for age
Plasma procalcitonin >2 SD above typical value for age

Haemodynamic
Arterial hypotension (SBP <90 mm Hg, MAP <70, or SBP reduction >40 mm Hg in adults or <2 SD below typical value for age)
SvO_2 >70%
Cardiac index >3·5 L/min per mol

Organ dysfunction
Arterial hypoxaemia (PaO_2/FiO_2<300)
Acute oliguria (urine output <0·5 mL/kg per h or 45 mmol/L for at least 2 h)
Creatinine increase >442 µmol/L
Coagulation abnormalities (INR >1·5 or aPTT >60 s)
Ileus (absent bowel sounds)
Thrombocytopenia (platelet count <100×10⁹ per L)
Hyperbilirubinaemia (plasma total bilirubin ≥70 mmol/L)

Tissue perfusion
Hyperlactataemia (>1 mmol/L)
Decreased capillary refill or mottling

SBP=systolic blood pressure. MAP=mean arterial blood pressure. SVO_2=mixed venous oxygen saturation. INR=international normalised ratio. aPPT=activated partial thromboplastin time. Information reproduced with permission from Levy, et al. SSCM/ESICM/ACCP/ATS/SIS International Sepsis Definitions Conference. *Crit Care Med* 2003; **31:** 1250–56 (table 1). Copyright 2003, Society of Critical Care Medicine.

FIGURE 2.2: The general diagnostic criteria used by clinicians to confirm if a patient has sepsis, and how many organ systems it has affected [4]. Figure re-printed from Brown et. al. [4].

Severe sepsis can lead to organ dysfunction, shock, and death in 35% of patients [4]. Multiple organ failure is a major threat to patients with severe sepsis, and the mortality rate is currently comparable to that of myocardial infarction [4]. The role of the innate immune system is to combat microbial infections but in the case of severe sepsis, over-activation of neutrophils significantly contributes to organ dysfunction within the microvasculature [7]. Figure 2.3 below shows the change in human neutrophil response to infection within a septic host and a severely septic host [3].

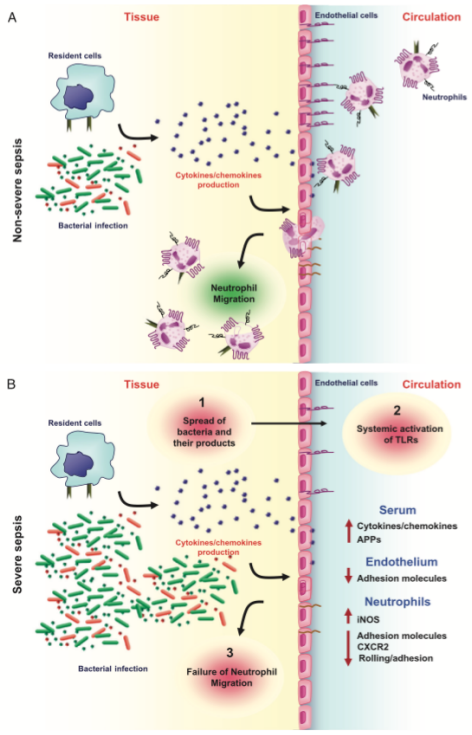

FIGURE 2.3: **A.** Neutrophil migration in non-severe sepsis. Pathogens induced TLR-4 activation, which induced the release of pro-inflammatory chemokines. P- and E-selectin induced on endothelial cells and L-selectin constitutively expressed on neutrophils facilitate initial binding and rolling on the endothelium. Chemokines on the endothelium activate integrins on neutrophils and result in firm adhesion. Neutrophils then extravasate through the endothelium to control the infection and repair tissue damage. **B.** Neutrophil impaired-migration in severe sepsis. The bacterial infection has spread and induced systemic TLR activation. The desensitization, or loss of, L-selectin activation by chemokines result in high levels of circulating pro-inflammatory cytokines. This inhibits neutrophil-endothelium interaction, which impacts the rolling, adhesion, and migration of neutrophils towards the infection [3]. Figure re-printed from Alves-Filho et. al. [3].

Patients with acute sepsis develop an accumulation of activated neutrophils within highly vascular organs, which puts the organ at high-risk for tissue damage [4]. Neutrophils are responsible for eliminating bacterial infections from the body, but neutrophil recruitment and migration to a site of infection is markedly decreased in septic subjects compared to healthy subjects [3]. There has been significant interest in studying the fundamental mechanisms governing neutrophil dysfunction in the presence of

sepsis. It is still unknown in the scientific and medical communities what mechanisms neutrophils utilize to contribute to the host immune response against sepsis.

Bacteria-derived lipopolysaccharide (LPS) is a potent activator of neutrophil function, and can block migration and adhesion to the endothelium [17]. Activation of neutrophils by bacteria-derived LPS contributes to the host response of septic shock as it results in increased plasticity and distinct phenotypic changes [1]. When LPS is released from bacterial cell walls, leukocytes and endothelial cells become activated, and induces the release of pro-inflammatory cytokines (interleukin-6, interleukin-1β, tumor necrosis factor α (TNFα)) [18]. This chemical response is known as septic shock in humans , which has a 40-60% mortality rate. Septic shock is characterized by tissue accumulation and activation of leukocytes. This inappropriate activation of neutrophils from bacteria-derived LPS results in a build up of cells and causes proteolytic tissue damage [15]. The interaction between L-selectin and the endothelium helps facilitate extravasation and accumulation of leukocytes in tissues, a key factor determinant of septic shock [18]. In the presence of LPS, the L-selectin-mediated adhesion of neutrophils to the endothelium is significantly impaired and L-selectin-mediated activation is significantly decreased. Figure 2.4 below shows how neutrophil recruitment differs in a healthy environment in comparison to a septic environment [4].

The β-1 integrin, VLA-4, has been identified on septic neutrophils and binds fibronectin and VCAM-1, indicating that neutrophils with β-1 and β-2 integrins are able to adhere to several vascular ligands [4]. This feature is significant because neutrophils are present in various microenvironments within the body. The flexibility and range of integrin-ligand binding combinations ensures neutrophil migration and adhesion to various tissues throughout the body.

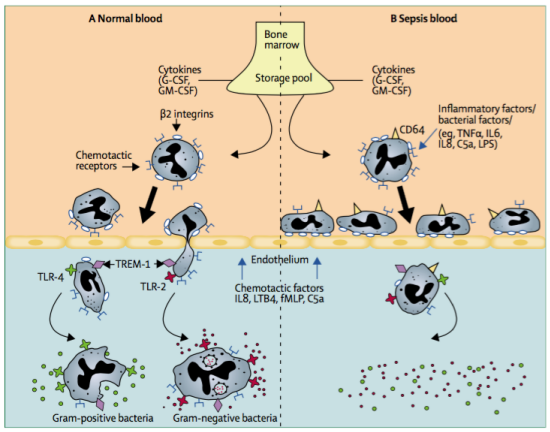

FIGURE 2.4: Cytokines are released in response to bacterial infections, which induce the release of neutrophils from circulation. **A.** In a healthy state, neutrophils enter sites of infection by adhering to the activated endothelium and migrating along a chemotactic gradient that is produced from the source of infection. **B.** In a septic state, neutrophils are stimulated with high levels of pro-inflammatory cytokines, which encourage the upregulation of surface integrins on neutrophils to promote firm adhesion to the endothelium. Additionally, these high levels of chemical stimuli downregulate the expression of chemokine receptors on neutrophils. This results in increased levels of firm adhesion to the endothelium and decreased response to chemical stimuli [4]. Figure re-printed from Brown et. al. [4].

Toll-like receptors (TLRs) are pattern recognition receptors that control the innate immune response to different microbial ligands [4]. Specifically, TLR4, is closely associated to the LPS receptor, CD14, and activation of this receptor downregulates neutrophil chemokine receptors, which can have a direct correlation to neutrophil response when over-activated by a septic host.

2.4 Prevalence of Sepsis

Sepsis manifests as a bacterial infection and can rapidly become life-threatening, and progress to multiple organ dysfunctions and death. Severe sepsis is defined as sepsis complicated by one or multiple debilitating organs. Patients with severe sepsis only make up 6-15% of the ICU population, but consume half of the ICU resources [5]. Due to the high need for resources the number of sepsis cases per year plays a crucial

role in hospital decision-making for infrastructure, equipment, and sufficient human resources. According to data collected by the Nationwide Inpatient Sample (NIS) in 1993-2003, the hospitalization rate for severe sepsis in the United States nearly doubled and population-based mortality rate increased by two thirds [5]. The hospitalization rate grew five times faster than what was originally predicted by Angus et. al., which can be attributed to increases in cancer, diabetes, obesity, and increased life expectancy for patients with chronic diseases [6]. As the number of cases continues to increase, there will be additional strain on hospital resources to ensure adequate care be provided to septic patients as well as other patients in the ICU.

2.5 Traction Force Microscopy

Traction Force Microscopy (TFM) is a powerful method used to quantify cell-material interactions to improve the understanding of cellular migration and adhesion. The Franck Lab utilizes a novel, large deformation formulation to quantify cellular displacement fields and traction stresses, described by Toyjanova, et. al. [9]. This unique approach reduces overall computation times by implementing the calculations on a personal computer's graphics processing unit (GPU) [10].

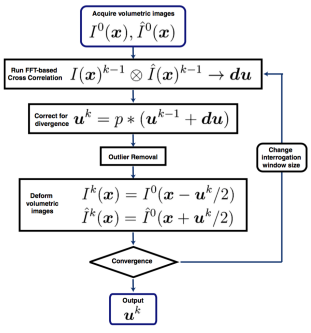

FIGURE 2.5: A flowchart of the FIDVC algorithm from obtaining the LSCM three-dimensional images to produce 3D material displacement fields [11]. Flowchart re-printed from Bar-Kochba et. al. [11].

Using three-dimensional imaging and traction force analysis (3D TFM) allows insight into various cellular processes. TFM produces cell-generated surface tractions

by using internal, measured, 3D cell-induced material displacement fields that are recorded using a fast iterative digital volume correlation (FIDVC) algorithm that tracks large deformation, described by Bar-Kochba et. al. [11]. The FIDVC algorithm achieves this in a user-friendly, high resolution, computationally efficient approach to detect large, non-linear deformation fields. Figure 2.5 above shows a flowchart of the FIDVC method to determine the displacement field provided by Bar-Kochba et. al. [11]. After using FIDVC to calculate the displacement fields, the surface tractions can be calculated using a forward formulation described by Franck et. al. [12,13].

The large deformation 3D TFM contains a fast iterative digital volume correlation (FIDVC) algorithm to compute the 3D cell-generated displacement fields from a series of laser scanning confocal microscopy (LSCM) 3D images. Then, the calculated 3D displacement fields are converted to cellular traction stresses using a large deformation continuum mechanics formulation [9]. The large deformation calculation uses a Neo-Hookean material behavior to model the experimental system, rather than prior formulations that assume small deformation, linear elastic materials. This large deformation approach has shown to adequately describe the material behavior of polyacrylamide at large strains [14].

2.5.1 Large Deformation

Since neutrophils can generate non-linear material strains, the calculations below account for large deformations as described by Toyjanova et. al. [9]. First, a point of the material undergoes a deformation from location **x** to location **y**, which can be represented by material displacement **u(x)** giving the following relationship:

$$y = x + u(x) \tag{2.1}$$

Differentiating with respect to **x** on both sides produces the following equation:

$$\Delta(y) = \Delta(x + u(x)) = I + \Delta(u(x)) = F \tag{2.2}$$

where **I** is the identity matrix and **F** is the material deformation gradient tensor. This tensor helps describe the shear and stretch of an infinitesimally small line segment **dx** as it moves a distance **u(x)**. Next, the Lagrangian strain tensor is used to calculate the material strains associated with the material deformation as follows:

$$E = 1/2(F^T \cdot F - I) \tag{2.3}$$

$$E = 1/2(\Delta u + (\Delta u)^T + \Delta u \cdot (\Delta u)^T) \tag{2.4}$$

which can be rewritten in the second equation in terms of the material displacement where $\Delta\mathbf{u}$ is the displacement gradient. The above equations are used in the case of large, homogeneous material deformation.

This 3D TFM technique uses the FIDVC algorithm to measure cell-imposed material displacement fields, and a large deformation continuum mechanics formulation to accurately calculate cell surface tractions. Figure 2.6 below depicts the large deformation, high resolution 3D TFM technique used to calculate displacement fields and traction stresses [11].

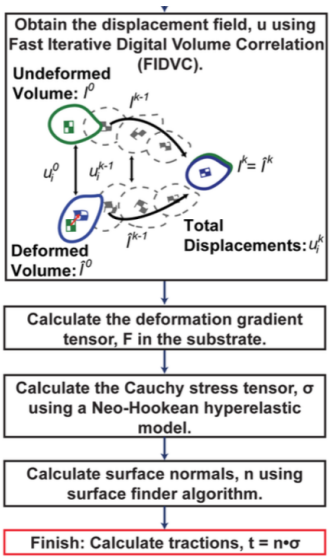

FIGURE 2.6: A flowchart representing the enhanced IDM to calculate the surface traction stresses from the material displacement fields [11]. Flowchart re-printed from Bar-Kochba et. al. [11].

2.5.2 Estimating Cellular Displacements

As described by Toyjanova et. al., the cellular deformation fields are calculated using a volumetric displacement finding scheme [9]. Using laser scanning confocal microscopy (LSCM), three-dimensional time-lapse z-stacks are captured of red fluorescent microspheres embedded in polyacrylamide hydrogel substrates. The motion of the embedded microspheres is tracked in three dimensions using the FIDVC algorithm described by Bar-Kochba et. al. [5]. This algorithm captures large material deformations by using a built-in iterative deformation method (IDM). The final results of using the FIDVC algorithm produces displacement fields with high spatial resolution, signal-to-noise, and fast computation times in comparison to previous DVC methods [13].

The following provides a brief description of the key technical steps of the FIDVC algorithm. To increase computation efficiency, the iterative deformation method (IDM) is extended into three dimensions and used to calculate volumetric displacement fields. The original IDM takes two volumetric images, $\mathbf{I}^0$ **and** $\widehat{I}^0$, and incrementally warps both

images by estimates of the cumulative displacement field $\mathbf{u}^k$ to linearize the deformation field between the images into k-increments. This begins by estimating the displacement field, $\mathbf{u}^0$, between the two volumetric images using the DVC cross-correlation formulation described by Franck et. al. [13]. Next, when k=1, the cumulative displacement field estimate shown below:

$$u^k = \Sigma u^{k-1} + \delta u \tag{2.5}$$

is used to symmetrically warp the undeformed and deformed images into as follows:

$$I^k(x) = I^0(x - u^k/2) \tag{2.6}$$

$$\widehat{I}^k(x) = \widehat{I}^0(x + u^k/2) \tag{2.7}$$

This DVC cross-correlation algorithm calculates the material displacement fields, $\mathbf{u}^k$, for each linearized k-increment for both deformed and undeformed images until they converge to the same intensity pattern, which produces the cumulative displacement field, $\mathbf{u}^k$. Figure 2.7 below shows the convergence scheme of the FIDVC algorithm, and a full description is provided by Bar-Kochba et. al. [11].

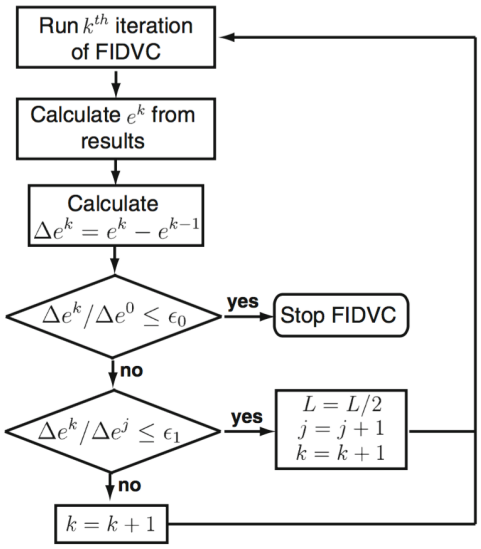

FIGURE 2.7: A flowchart depicting the convergence scheme using in the FIDVC algorithm [11]. Flowchart re-printed from Bar-Kochba et. al. [11].

2.5.3 Estimating Cellular Tractions

The deformation gradient tensor, **F**, is calculated after finding the cellular displacement fields $\mathbf{u}^k$. The displacement gradient, $\Delta\mathbf{u}$, and the deformation gradient tensor, **F**, are directly related to the gradients of the measured displacement field.

The first step in calculating the cellular surface tractions is to determine the material's true stress tensor, or Cauchy stress σ. The following calculations noted are specific to polyacrylamide and a Neo-Hookean material model. The Cauchy stress, σ, is as follows:

$$\sigma = (\mu/J^{5/3})(B - 1/3trace(B) \cdot I) + K(J-1)I \tag{2.8}$$

where μ and K are the shear and bulk moduli of the material. The following equations show the relationship of the shear and bulk moduli to the Young's modulus, E, of a material:

$$K = E/(3(1-2\nu)), \mu = E/(2(1+\nu)) \tag{2.9}$$

Next, use the deformation gradient tensor, **F**, to determine the Jacobian of **F**, **J**, and the left Cauchy Green tensor, **B**:

$$J = det(F), B = F \cdot F^T \tag{2.10}$$

Then using the Cauchy relations, calculate the surface tractions as follows:

$$t = n \cdot (\sigma) \tag{2.11}$$

where **n** is the surface normal in the deformed state, which can be determined by tracking the fluorescent microspheres in the LSCM images. Using the FIDVC algorithm and 3D TFM technique, the surface tractions can then be calculated using the same method of finding the surface normal and the Cauchy relation above.

As strains and material constants must be considered when determining the surface tractions, the large deformation 3D TFM technique has been tested to ensure high resolution and measurement sensitivity. This method can resolve displacements and strains greater than 0.5 μm and 1.0%, which relates to stresses and traction forces greater than 50 Pa and 50 pN/μm^2 [9].

Chapter 3

Materials and Methods

More detailed protocols for the following experimental setup can be found in Appendix A.

3.1 Glass coverslips surface modification

Prepare hydrophobic coverslips

Circular 25 mm glass coverslips (Fisher Scientific, Waltham, MA) were chemically modified to create a hydrophobic surface and promote easy detachment from the polyacrylamide hydrogels. The glass coverslips were placed in a glass Petri dish containing a solution of 97% (v/v) hexane (Fisher Scientific, Waltham, MA), 2.5% (v/v) (tridecafluoro-1,1,2,2-tetrahydrooctyl)-triethoxysilane (SIT) (Gelest, Morrisville, PA), and 0.5% (v/v) acetic acid (Sigma-Aldrich, St. Louis, MO) for 5 minutes. The activated glass coverslips were removed and left to dry [19].

Prepare hydrophilic coverslips

Circular 25 mm glass coverslips were surface modified to promote covalent bonding to polyacrylamide hydrogels. The glass coverslips were rinsed in ethanol and placed in a glass Petri dish containing a solution of 0.5% (v/v) 3-aminopropyltriethoxysilane (APTS) (Sigma-Aldrich, St. Louis, MO) in ethanol for 5 minutes. Next, the glass coverslips were rinsed in ethanol and placed in a glass Petri dish containing a solution of 0.5% glutaraldehyde (Polysciences, Inc., Warrington, PA) in deionized water for 30 minutes. The activated glass coverslips were rinsed in DI water, and left to dry in 30°C oven for at least 30 minutes [20].

3.2 Preparation of polyacrylamide hydrogels

The protocol for tunable polyacrylamide hydrogels to study neutrophil force generation is adapted from by Tse and Engler [21].

The polyacrylamide (PA) hydrogels were prepared from acrylamide (40% w/v, Bio-Rad Laboratories, Hercules, CA) and *N,N*-methylene-bis-acrylamide (BIS, 2%, w/v, Bio-Rad Laboratories, Hercules, CA) stock solutions [12]. To make 1.7 kPa PA hydrogels, the concentrations for acrylamide and BIS were chosen to be 3%/0.225%, and 5%/0.300% to make 8.7 kPa hydrogels. Polymerization was initiated by adding ammonium persulfate (Sigma-Aldrich, St. Louis, MO) and *N,N,N,N*-tetramethylethylenediamine (Life Technologies, Grand Island, NY). The solution was vortexed for 30 seconds, and the PA solution was pipetted on the hydrophilic glass coverslip and sandwiched with a hydrophobic glass coverslip. The PA hydrogel was submerged in deionized water and allowed to finish polymerizing and hydrate for 45 minutes. After the hydrophobic coverslip was removed, the PA hydrogel was functionalized with sulfo-SANPAH (Thermo Fisher Scientific, Waltham, MA) - a bifunctional crosslinker [12,20]. Then, sulfo-SANPAH was deposited on the surface of each PA hydrogel and exposed to UV light for 15 minutes. The darkened sulfo-SANPAH was removed with gentle aspiration and the UV radiation repeated with fresh sulfo-SANPAH solution. Next, the PA hydrogels were thoroughly rinsed with 1X PBS and functionalized with a solution of human protein. The two proteins used were human fibronectin and human ICAM-1, to study the cellular response to different protein coatings that mimic different microenvironments in the body. Table 3.1 below shows the percent volume required to create the desired elastic modulus of the polyacrylamide hydrogel [21].

TABLE 3.1: The percent volume requirements to make tunable 1.7 kPa and 8.7 kPa polyacryalmide hydrogels.

Elastic Modulus (kPa)	**Acrylamide % (v/v)**	**Bis % (v/v)**	**Beads % (v/v)**
1.67 +/- 0.14	3	0.225	10.00
8.73 +/- 0.79	5	0.300	10.00

TABLE 3.2: The percent volume requirements to make tunable 1.7 kPa and 8.7 kPa polyacryalmide hydrogels.

Elastic Modulus (kPa)	**Acrylamide % (v/v)**	**Bis % (v/v)**	**Beads % (v/v)**
1.67 +/- 0.14	3	0.225	10.00
8.73 +/- 0.79	5	0.300	10.00

3.3 Protein functionalization on polyacrylamide hydrogels

Human fibronectin was coated on the PA hydrogel at a concentration of 0.2 mg/mL and human ICAM-1 at a concentration of 50 μg/mL. The protein functionalization was left undisturbed at 4°C overnight. The next day, the PA hydrogel substrates were rinsed twice in 1X PBS, sterilized with UV radiation for 10 minutes, and placed in chamlide chamber with 1 mL solution of L-15 and 2 mg/mL glucose for imaging.

3.4 Human neutrophil isolation

The protocol for human neutrophil isolation follows the EasySep Direct Human Neutrophil Isolation Kit, which is designed to isolate functional, highly purified human neutrophils from whole blood by immunomagnetic negative selection [21]. This kit targets non-neutrophils in the whole blood to remove by using antibodies that recognize specific cell surface markers. The use of the Isolation Cocktail and RapidSpheres^{TM} tags the cells with monoclonal antibodies and removes them with magnetic particles when the sample is placed in the EasySep magnet [21].

3.5 Live cell imaging

Using a Nikon A-1 confocal system mounted on a TI Eclipse inverted optical microscope controlled by NI-Elements Nikon Software, three-dimensional image stacks of multiple x-y positioned cells were captured to analyze displacement fields and traction forces [19]. A 40X water immersion objective mounted on a TI Z-Drive positioner was

used for all experiments. Red 0.5 μm fluorescent microspheres were embedded into the PA hydrogel and excited with a red 580 nm laser. To ensure physiological imaging conditions, an imaging chamber maintained a temperature of 37°C for the extent of the experiment. The cell membrane was fluorescently dyed with a green actin-based dye and excited with an Argon 488 nm laser. About 50,000 isolated human neutrophils were primed with 1 nM fMLP and then plated on the polyacrylamide hydrogel, and allowed to settle for 30 minutes. One media exchange before imaging removed free-floating cells and kept the spread neutrophils for easier x-y selection.

Chapter 4

Results and Discussion

4.1 Neutrophil force generation in response to LPS activation

This project focused on analyzing the change in neutrophil displacement fields and traction stresses in response to the addition of 200 ng/mL LPS. Human neutrophils were studied on 1.7 kPa and 8.7 kPa polyacrylamide hydrogels, coated with either 50 μg/mL human ICAM-1 or 200 μg/mL human fibronectin. These conditions created a test chart as follows:

TABLE 4.1: A test chart outlining the different conditions in this thesis project.

1.7 kPa	**ICAM, no LPS**	**ICAM, LPS**	**Fn, no LPS**	**Fn, LPS**
8.7 kPa	ICAM, no LPS	ICAM, LPS	Fn, no LPS	Fn, LPS

Using the FIDVC algorithm described by Bar-Kochba et. al. and the large deformation 3D TFM technique described by Toyjanova et. al., the displacement fields and traction stresses were calculated and compared to analyze the change in neutrophil migration and adhesion as it depends on stiffness, ligand, and presence of LPS [9,11]. Table 4.2 below shows the change in material displacement fields in all three dimensions and surface traction stresses before and after LPS activation. The values were computed by taking the difference between maximum displacement and traction after LPS activation from maximum displacement and traction before LPS activation. There is a significant amount of negative values in the table, indicating there was a decrease in displacement and traction following 200 ng/mL LPS activation.

The addition of LPS decreased the average displacement field in the x-y direction, regardless of stiffness of polyacrylamide gel or protein coating. The displacement field

TABLE 4.2: The change in maximum and minimum displacement fields and maximum surface traction stresses for all four conditions as it relates to LPS activation. Additionally, the average noise floor in each direction for each experimental condition. All displacement in μm, and traction in Pa.

Difference	**Max X-Y Disp**	**Max Z Disp**	**Min Z Disp**	**Max Traction**
1.7 kPa, ICAM	-0.03599	-0.06146	-0.01824	-185.959
1.7 kPa, Fn	-0.03461	-0.04962	0.07612	-137.791
8.7 kPa, ICAM	-0.09559	-0.07189	0.00679	-948.993
8.7 kPa, Fn	-0.02272	0.033483	-0.00884	-289.494

in x-y decreased an average of 0.1 μm with average noise of 0.03 μm, indicating minimal dysregulation in cell mechanics.

LPS activation did not have a significant effect on displacement in the z-direction as the average difference was -0.008 μm pulling up on the polyacrylamide and 0.07 μm pushing into the polyacrylamide, with noise of 0.05 μm. Therefore, it can be assumed that human neutrophil displacement does not vary in response to the addition of LPS. However, it would be interesting to use TURF imaging to further analyze the change in cytoskeletal properties and integrin presence on the surface of the neutrophil as it responds to LPS. There may require a higher concentration of LPS to adequately mimic a septic host environment.

LPS activation of neutrophils significantly decreased surface traction stresses, regardless of polyacrylamide stiffness or protein coating. The comparison of human neutrophil displacement fields and traction forces before and after LPS activation can be seen in the tables below.

Tables 4.3 and 4.4 below show the average maximum and minimum material displacement fields in all three dimensions and the maximum surface traction stresses exhibited by human neutrophils on 1.7 kPa and 8.7 kPa polyacrylamide hydrogels coated with 50 μg/mL ICAM-1. There was no significant change in the calculated displacement fields for all three directions, as maximum x-y displacement stayed near 0.3 μm, maximum z-direction at 0.5 μm, and minimum z-direction at -0.3 μm. The surface

traction stresses decreased regardless of polyacrylamide stiffness, but the Elastic Modulus played a significant role in determining initial applied surface traction stress. The 1.7 kPa polyacrylamide hydrogel produced neutrophil surface traction stresses in the range of 450 Pa to 700 Pa, whereas the 8.7 kPa polyacrylamide hydrogel produced significantly larger surface traction stresses in the range of 1500 Pa to 2500 Pa. This represents a high level of dependence on substrate stiffness as it relates to traction stresses, but nearly zero dependence for material displacement fields.

TABLE 4.3: The average displacement fields and surface traction stresses for 1.7 kPa and 8.7 kPa polyacrylamide hydrogels coated with 50 μg/mL ICAM-1 before LPS activation. All displacements in μm, and tractions in Pa.

ICAM, Before LPS	Max X-Y Disp	Max Z Disp	Min Z Disp	Max Traction
1.7 kPa	0.2697	0.55992	-0.25145	673.1249
8.7 kPa	0.25836	0.52006	-0.30525	2539.265

TABLE 4.4: The average displacement fields and surface traction stresses for 1.7 kPa and 8.7 kPa polyacrylamide hydrogels coated with 50 μg/mL ICAM-1 after 200 ng/mL LPS activation. All displacements in μm, and tractions in Pa.

ICAM, After LPS	Max X-Y Disp	Max Z Disp	Min Z Disp	Max Traction
1.7 kPa	0.23371	0.49846	-0.26969	487.1656
8.7 kPa	0.16726	0.44818	-0.29844	1590.272

Tables 4.5 and 4.6 below show the average maximum and minimum material displacement fields in all three dimensions and the maximum surface traction stresses exhibited by human neutrophils on 1.7 kPa and 8.7 kPa polyacrylamide hydrogels coated with 200 μg/mL fibronectin. There was no significant change in the calculated displacement fields for all three directions, as maximum x-y displacement stayed near 0.3 μm for 1.7 kPa and 0.18 μm for 8.7 kPa, maximum z-direction at 0.5 μm for 1.7 kPa and 0.4 μm for 8.7 kPa, and minimum z-direction at -0.3 μm for both stiffnesses. This demonstrates a slight variance in material displacement fields as the substrate stiffness

changes, but not a large enough difference to overcome the average noise floor in each experiment. This is further explained below in 4.3 Noise Calculation.

TABLE 4.5: The average displacement fields and surface traction stresses for 1.7 kPa and 8.7 kPa polyacrylamide hydrogels coated with 200 μg/mL ICAM-1 fibronectin before LPS activation. All displacements in μm and tractions in Pa.

Fn, Before LPS	**Max X-Y Disp**	**Max Z Disp**	**Min Z Disp**	**Max Traction**
1.7 kPa	0.28486	0.53161	-0.35145	499.9828
8.7 kPa	0.179446	0.380142	-0.27713	1583.334

TABLE 4.6: The average displacement fields and surface traction stresses for 1.7 kPa and 8.7 kPa polyacrylamide hydrogels coated with 200 μg/mL ICAM-1 fibronectin after 200 ng/mL LPS activation. All displacements in μm, and tractions in Pa.

Fn, After LPS	**Max X-Y Disp**	**Max Z Disp**	**Min Z Disp**	**Max Traction**
1.7 kPa	0.25025	0.48199	-0.27533	362.1909
8.7 kPa	0.16026	0.42533	-0.28839	1323.195

The surface traction stresses decreased regardless of polyacrylamide stiffness, but the Elastic Modulus played a significant role in determining initial applied surface traction stress. The 1.7 kPa polyacrylamide hydrogel produced neutrophil surface traction stresses in the range of 350 Pa to 500 Pa, whereas the 8.7 kPa polyacrylamide hydrogel produced significantly larger surface traction stresses in the range of 1300 Pa to 1600 Pa. This represents a high level of dependence on substrate stiffness as it relates to traction stresses, but nearly zero dependence for material displacement fields. Interestingly, the surface traction stresses for each polyacrylamide stiffness were larger when coated with ICAM-1 than fibronectin. This is different than what was originally hypothesized. As the ECM is inherently stiffer than the endothelium, it would make sense that neutrophils inherently know to relate fibronectin with a stiffer substrate than ICAM-1. This could be a key find in further understanding the biomechanical changes that the immune system undergoes in the presence of sepsis.

Figures 4.1-4.3 below show a z-slice of the cell membrane dyed neutrophil in a 1.7 kPa polyacrylamide hydrogel with 0.5 μm red fluorescent microspheres, coated with 50 μg/mL ICAM-1. Additionally, using the FIDVC algorithm and LD 3D TFM technique, the figures show material displacement field plots in the x-y direction and z-direction, and the surface traction stresses. Figure 4.1 displays the neutrophils calculations before LPS activation, Figure 4.2 is immediately after LPS activation, and Figure 4.3 is 30 minutes after LPS activation. Though there is not a significant change in material displacement fields in response to LPS activation, it is clear that the neutrophil is pulling the gel inwards by probing with its pseudopods on the polyacrylamide and pulling upwards as displayed. The neutrophil consistently applies surface traction stress throughout the experiment, though it does significantly decrease as a result of LPS activation.

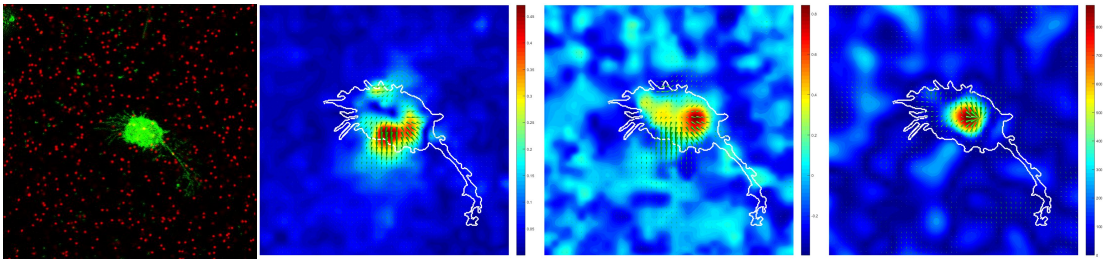

FIGURE 4.1: (left-right) Green cell z-slice and red 0.5 μm fluorescent microspheres in 1.7 kPa polyacrylamide hydrogel coated with 50 μg/mL ICAM-1; Material displacement fields in x-y direction and z-direction (μm); and traction stresses (Pa). All data points taken before LPS activation.

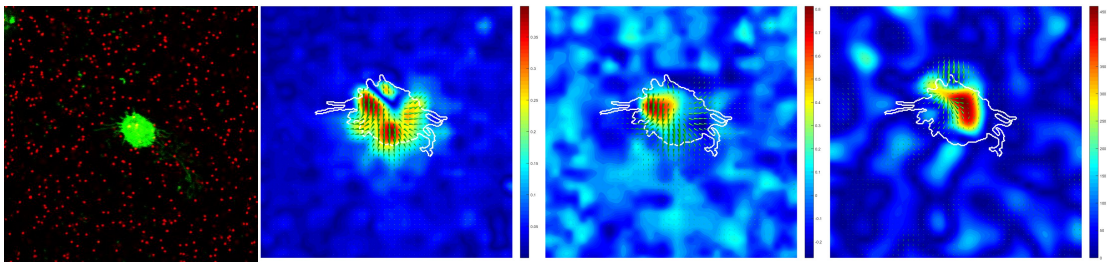

FIGURE 4.2: (left-right) Green cell z-slice and red 0.5 μm fluorescent microspheres in 1.7 kPa polyacrylamide hydrogel coated with 50 μg/mL ICAM-1; Material displacement fields in x-y direction and z-direction (μm); and traction stresses (Pa). All data points taken immediately after 200 ng/mL LPS activation.

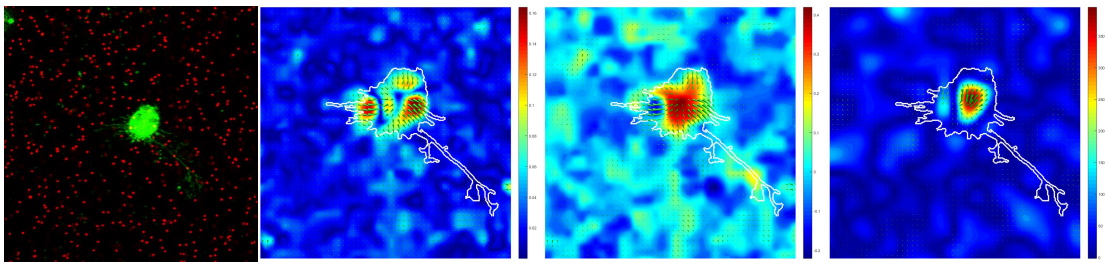

FIGURE 4.3: (left-right) Green cell z-slice and red 0.5 μm fluorescent microspheres in 1.7 kPa polyacrylamide hydrogel coated with 50 μg/mL ICAM-1; Material displacement fields in x-y direction and z-direction (μm); and traction stresses (Pa). All data points taken 30 minutes after 200 ng/mL LPS activation.

Figures 4.4 and 4.5 below show a z-slice of the cell membrane dyed neutrophil in a 1.7 kPa polyacrylamide hydrogel with 0.5 μm red fluorescent microspheres, coated with 200 μg/mL fibronectin. Also included are material displacement field plots in the x-y direction and z-direction, and the surface traction stresses. Figure 4.4 represents the neutrophils state on the polyacrylamide hydrogel before LPS activation, and Figure 4.5 is 30 minutes after 200 ng/mL LPS activation. This system presented quite a bit of noise in the z-direction and surface traction stresses plot. This can be due to thermal drift or human error during the experimental setup, which is discussed more in 4.3 Noise Calculation. This experiment shows distinct material displacement fields before

LPS activation, and unclear traction stresses due to an increased level of noise. Additionally, the displacement field in the x-y direction after LPS activation seems minimal in reference to the noise, whereas the neutrophil is distinctly pulling up on the polyacrylamide after activation even with an increase in noise.

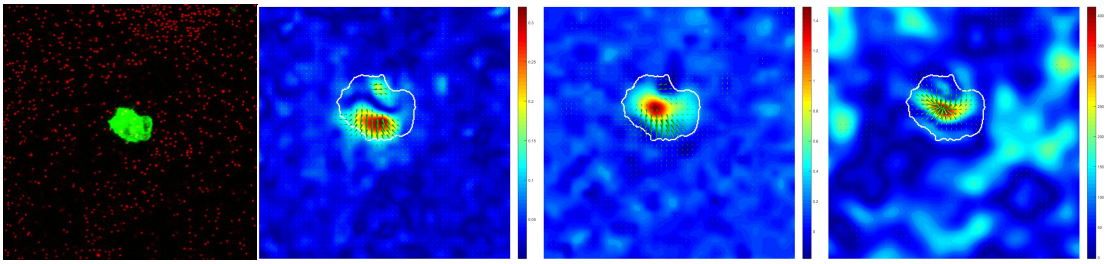

FIGURE 4.4: (left-right) Green cell z-slice and red 0.5 μm fluorescent microspheres in 1.7 kPa polyacrylamide hydrogel coated with 200 μg/mL fibronectin; Material displacement fields in x-y direction and z-direction (μm); and traction stresses (Pa). All data points taken before LPS activation.

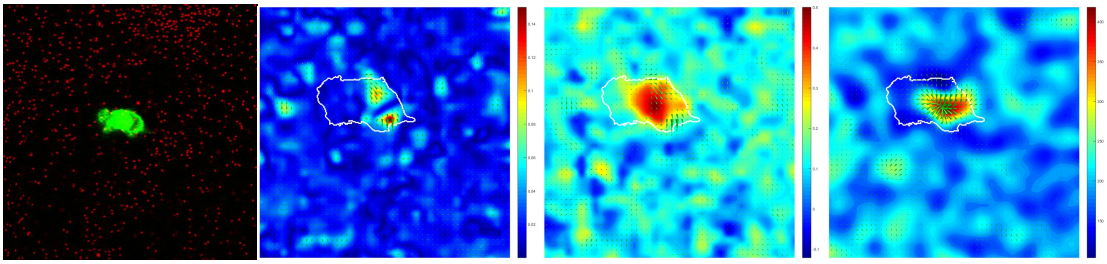

FIGURE 4.5: (left-right) Green cell z-slice and red 0.5 μm fluorescent microspheres in 1.7 kPa polyacrylamide hydrogel coated with 200 μg/mL fibronectin; Material displacement fields in x-y direction and z-direction (μm); and traction stresses (Pa). All data points taken 30 minutes after 200 ng/mL LPS activation.

4.2 Neutrophil force generation in response to polyacrylamide hydrogel stiffness and protein coating

Human neutrophils were highly responsive to the polyacrylamide stiffness and protein. By analyzing the tables below, neutrophils exerted significantly larger surface

tractions the stiffer the polyacrylamide, with a 4X increase. This data is only comparing the change in neutrophil force generation as it depends on polyacrylamide stiffness, so values below are all taken before LPS activation. The significant change in magnitude of surface traction stresses as it depends on polyacrylamide stiffness relates to the neutrophil's ability to alter its force generation as it relates to its environment This is key in studying both rolling and adhesion to the endothelium and transmigration to the site of injury. This finding requires further investigation to determine if this is a significant factor in better understanding the mechanical dysregulation of neutrophils in a septic host.

There was a drastic change in human neutrophil displacement fields and traction stresses between plating on human ICAM-1 and human fibronectin. This can be expected because neutrophils sense their surroundings and use both β-1 and β-2 integrins in the steps of the recruitment cascade to bind to ICAM-1 and fibronectin, as ICAM-1 mimics the crawling, adhesion, and arrest to the endothelium whereas fibronectin is present after extravasation into the extracellular matrix. Tables 4.7 and 4.8 below show the maximum displacement fields in the x-y and z-directions and maximum traction forces applied, as it changes relative to protein coating and polyacrylamide stiffness. This data is only comparing the change in neutrophil force generate as it depends on stiffness and protein, so values below are all taken before LPS activation.

TABLE 4.7: The average displacement fields and surface traction stresses for 1.7 kPa polyacrylamide hydrogels before LPS activation. All displacements in μm, and tractions in Pa.

1.7 kPa, Before LPS	**Max X-Y Disp**	**Max Z Disp**	**Min Z Disp**	**Max Traction**
ICAM	0.26970	0.55992	-0.25145	673.1249
Fn	0.28486	0.53161	-0.35145	499.9828

The following Figures 4.6-4.10 represent data from neutrophils on 8.7 kPa polyacrylamide hydrogels coated with either 50 μg/mL ICAM-1 or 200 μg/mL fibronectin. Figures 4.6 and 4.7 shows the material displacement fields in three dimensions and surface traction stresses for neutrophils on 200 μg/mL fibronectin before and after 200 ng/mL

TABLE 4.8: The average displacement fields and surface traction stresses for 8.7 kPa polyacrylamide hydrogels before LPS activation. All displacements in μm and tractions in Pa.

8.7 kPa, Before LPS	**Max X-Y Disp**	**Max Z Disp**	**Min Z Disp**	**Max Traction**
ICAM	0.25836	0.52006	-0.30525	2539.265
Fn	0.17946	0.38014	-0.27713	1583.334

LPS activation. This data shows a significant amount of noise in the material displacement field in the z-direction before LPS activation and the surface traction stress after LPS activation. This is important to consider because calculations for displacement and traction may be due to noise in the system, rather than mechanical properties exerted by the neutrophil. However, given the noise calculations conducted for each experiment and further explained in 4.3 Noise Calculation, though there is significant noise visually there is still an increase in displacement and stress around the cell which is attributed to neutrophil mechanics on 8.7 kPa.

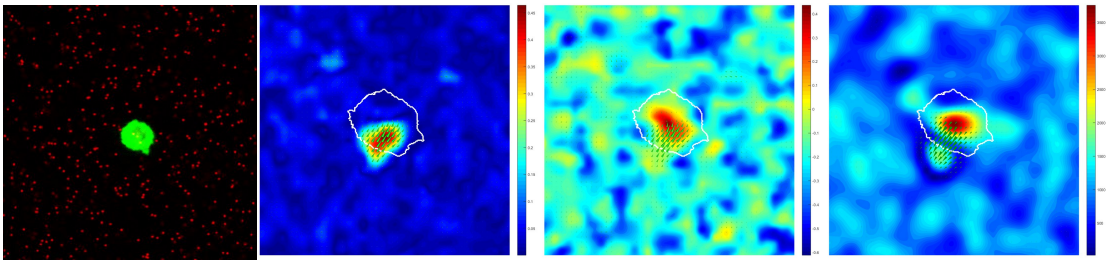

FIGURE 4.6: (left-right) Green cell z-slice and red 0.5 μm fluorescent microspheres in 8.7 kPa polyacrylamide hydrogel coated with 200 μg/mL fibronectin; Material displacement fields in x-y direction and z-direction (μm); and traction stresses (Pa). All data points taken before LPS activation.

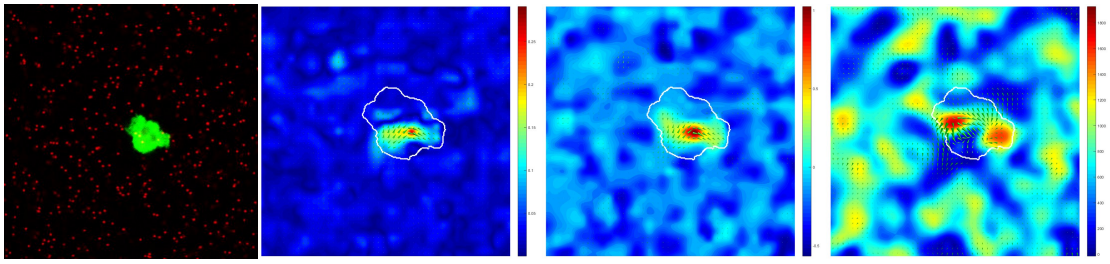

FIGURE 4.7: (left-right) Green cell z-slice and red 0.5 μm fluorescent microspheres in 8.7 kPa polyacrylamide hydrogel coated with 200 μg/mL fibronectin; Material displacement fields in x-y direction and z-direction (μm); and traction stresses (Pa). All data points taken immediately after 200 ng/mL LPS activation.

Figures 4.8-4.10 show neutrophil displacement and tractions before and after LPS activation. Figure 4.8 is a very good representation of high signal-to-noise in the experimental setup, and clear bead displacement around the edges of the cell for x-y direction and directly underneath the entire cell for z-direction. The traction stresses immediately and 30 minutes after LPS activation show a low signal-to-noise, indicating that the values calculated for the neutrophil may be attributed to a higher level of noise in the system rather than the mechanics of the cell.

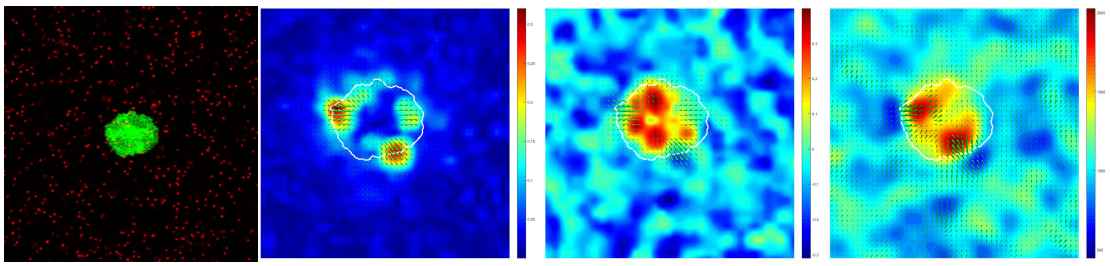

FIGURE 4.8: (left-right) Green cell z-slice and red 0.5 μm fluorescent microspheres in 8.7 kPa polyacrylamide hydrogel coated with 50 μg/mL ICAM-1; Material displacement fields in x-y direction and z-direction (μm); and traction stresses (Pa). All data points taken before LPS activation.

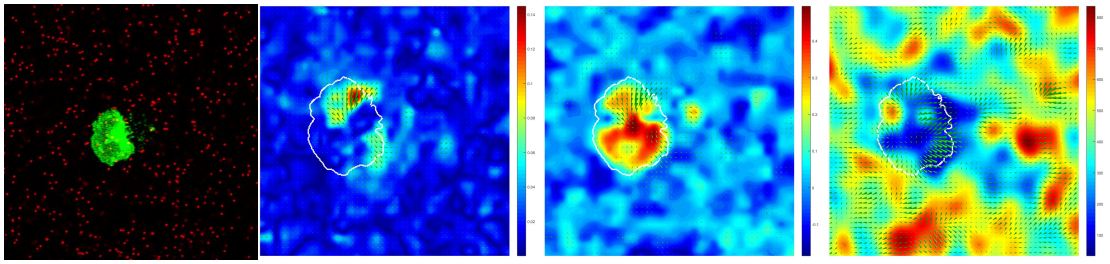

FIGURE 4.9: (left-right) Green cell z-slice and red 0.5 μm fluorescent microspheres in 8.7 kPa polyacrylamide hydrogel coated with 50 μg/mL ICAM-1; Material displacement fields in x-y direction and z-direction (μm); and traction stresses (Pa). All data points taken immediately after 200 ng/mL LPS activation.

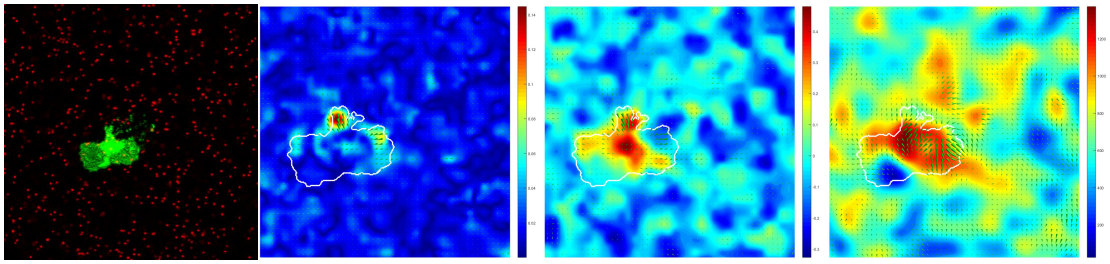

FIGURE 4.10: (left-right) Green cell z-slice and red 0.5 μm fluorescent microspheres in 8.7 kPa polyacrylamide hydrogel coated with 50 μg/mL ICAM-1; Material displacement fields in x-y direction and z-direction (μm); and traction stresses (Pa). All data points taken 30 minutes after 200 ng/mL LPS activation.

Figure 4.11 represents the same neutrophil as shown in Figures 4.8-4.10 above, shown on a cone plot to represent x-y-z displacement in one graph. Additionally, the noise has been significantly reduced in this system to highlight the increased level of displacement fields around the neutrophil. This aids in better visualization of the displacement fields that are attributed to neutrophil mechanics, while negating the noise in the system.

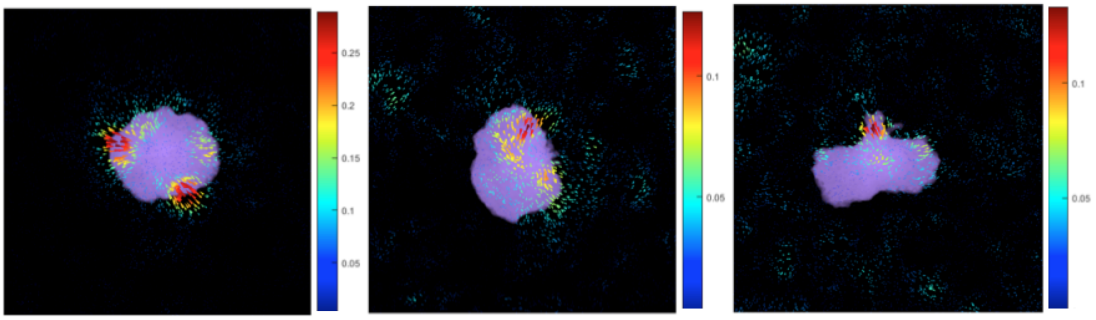

FIGURE 4.11: Calculated material displacement fields in three dimensions shown on one cone plot, with data in μm. (left-right) Before LPS activation; Immediately after 200 ng/mL LPS activation; After 200 ng/mL LPS activation.

Given the above findings, it can be seen that neutrophils exert much larger traction forces on fibronectin than ICAM-1. In addition, the stiffness of polyacrylamide has a direct effect on the magnitude of applied traction stresses. When neutrophils are plated on fibronectin-coated or ICAM-coated polyacrylamide hydrogels, the applied traction force decreases significantly regardless of stiffness. The change in x-y and z-directions of displacement fields are minimal between before and after LPS activation, as the largest change is roughly 0.1 μm with approximate 0.01-0.08 μm noise floor in each direction.

4.3 Noise Calculation

It is key to account for noise in the experimental system as this project focused on analyzing neutrophils response to changes in substrate stiffness, protein coating, and LPS activation. Noise could be due to thermal drift during the experiment, imperfection in using the TI Z-Drive on the confocal microscope, or human error in conducting the experiment. Table 4.9 below shows average noise in three dimensions and Table 4.10 shows the average signal-to-noise ratio in an experiment.

TABLE 4.9: The average noise floor in three dimensions for a LD 3D TFM experiment testing 1.7 kPa and 8.7 kPa polyacrylamide hydrogels coated with 200 μg/mL fibronectin.

Elastic Modulus (kPa)	**Max X Noise (μm)**	**Max Y Noise (μm)**	**Max Z Noise (μm)**
1.7 kPa	0.020076	0.021399	0.083972
8.7 kPa	-0.060029	0.034548	-0.025375

TABLE 4.10: The average signal-to-noise in three dimensions for a LD 3D TFM experiment testing 1.7 kPa and 8.7 kPa polyacrylamide hydrogels coated with 200 μg/mL fibronectin.

Elastic Modulus (kPa)	**Max X-Y Disp (μm)**	**Max Z Disp (μm)**	**Min Z Disp (μm)**
1.7 kPa	0.0861	0.27327	-0.18173
8.7 kPa	0.10685	0.13055	-0.11453

Figure 4.12 below shows a typical average noise floor in all three dimensions before LPS activation, and Figure 4.13 shows the same experimental setup 30 minutes after 200 ng/mL LPS activation. The x- and y-directions represent a Gaussian curve, while the z-direction tends to have an increased level of noise due to the imperfection in the TI Z-Drive and confocal microscope system. The z-direction presents an imperfect Gaussian, or bimodal curve in some experiments. The noise floor histograms are a good indication of understanding the average noise in that experimental setup, which will be a good determinant to understand if the calculated material displacement fields and surface traction stresses are due to increased noise or generated from the neutrophil.

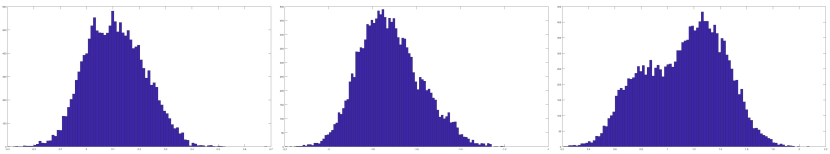

FIGURE 4.12: (left-right) Noise in x-direction; Noise in y-direction, and Noise in z-direction. Three noise floor histograms depicting average noise in three dimensions on a 1.7 kPa polyacrylamide hydrogel coated with 200 μg/mL fibronectin before LPS activation.

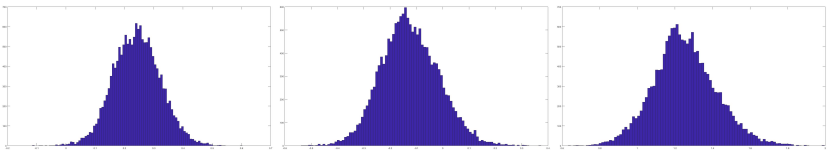

FIGURE 4.13: (left-right) Noise in x-direction; Noise in y-direction, and Noise in z-direction. Three noise floor histograms depicting average noise in three dimensions on a 1.7 kPa polyacrylamide hydrogel coated with 200 μg/mL fibronectin after 200 ng/mL LPS activation.

Figures 4.14 and 4.15 below show an experiment with an increased level of noise. Figure 4.14 shows the average noise floor in three dimensions before LPS activation, and Figure 4.15 shows the average noise floor of the same experimental setup 30 minutes after 200 ng/mL LPS activation. The wider Gaussian curve in the x- and y-directions, and the bimodal curve in the z-direction indicate a significant amount of noise in this system. It is important to analyze the noise floor in each experimental setup as each polyacrylamide hydrogel can produce a variance of imperfections and noise. This directly impacts the FIDVC algorithm and LD 3D TFM technique when calculating the material displacement fields and surface traction stresses. The greater the noise, the less convincing the calculated displacement fields are to be produced from the cell rather than additional noise.

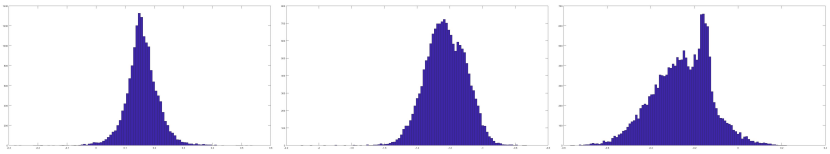

FIGURE 4.14: (left-right) Noise in x-direction; Noise in y-direction, and Noise in z-direction. Three noise floor histograms depicting average noise in three dimensions on a 8.7 kPa polyacrylamide hydrogel coated with 200 μg/mL fibronectin before LPS activation.

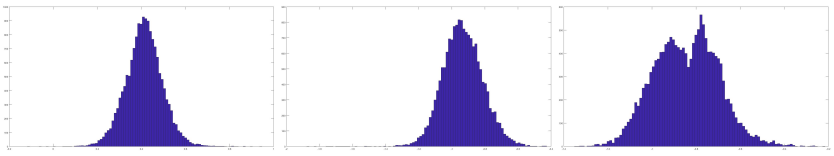

FIGURE 4.15: (left-right) Noise in x-direction; Noise in y-direction, and Noise in z-direction. Three noise floor histograms depicting average noise in three dimensions on a 8.7 kPa polyacrylamide hydrogel coated with 200 μg/mL fibronectin after 200 ng/mL LPS activation.

Chapter 5

Conclusion

This project focused on better understanding the mechanical dysregulation of human neutrophils when activated by bacteria-derived LPS. Using 200 ng/mL LPS did not produce a significant change in material displacement fields, as was originally hypothesized. However, there was a significant decrease in surface traction stresses in the presence of LPS, regardless of polyacrylamide stiffness or protein coating. This could be due to the effect of LPS on the neutrophils mechanosensing genes, which are a key part in the neutrophils ability to adapt to various environments in the body.

Additionally, this project studied the reliance of neutrophil mechanics on polyacrylamide stiffness and protein coating. The endothelium is inherently softer than the ECM, so studying two stiffnesses and two ligands revealed a greater dependence on stiffness than ligand. Surface traction stresses were markedly smaller on the softer polyacrylamide, indicating that neutrophils mechanosensing abilities are considered above their chemical sensing in a hierarchy.

Moving forward, additional experiments would need to be conducted in order to further understand the effect of LPS on neutrophil force generation with regards to displacement fields and traction forces. Utilizing the FIDVC algorithm and large deformation 3D TFM technique has allowed for precise resolution of bead displacements from 0.5 μm upwards. In addition, it is clear that human neutrophils can sense their surrounding environment and alter their response by changing magnitude of applied traction. The stiffer the polyacrylamide hydrogel, the larger the traction forces. In addition, neutrophils exert significantly larger tractions on fibronectin than ICAM-1 which can be tied to the presence of fibronectin in the ECM after the neutrophil has extravasated from the endothelium and is migrating towards the site of inflammation. ICAM-1 is utilized primarily for crawling, adhesion, and arrest on the endothelium

which is known to have a much softer stiffness than the surrounding ECM.

The findings from this project can help to better understand neutrophil response to change in stiffness and protein to mimic location and environment in the body, as well as LPS activation to study healthy and septic neutrophils. Further studying at a cellular level can help to better understand neutrophil dysregulation, and solutions to provide therapy in the case of sepsis, and other autoimmune diseases.

Chapter 6

References

[1] Kolaczkowska, Elzbieta, and Paul Kubes. “Neutrophil Recruitment and Function in Health and Inflammation.” Nature Reviews Immunology, vol. 13, no. 3, Mar. 2013, pp. 159–175., doi:10.1038/nri3399.

[2] Guck, Jochen, et al. “Critical Review: Cellular Mechanobiology and Amoeboid Migration.”Integrative Biology, vol. 2, no. 11-12, 2010, p. 575., doi:10.1039/c0ib00050g.

[3] J. C. Alves-Filho, A. de Freitas, F. Spiller, F. O. Souto, F. Q. Cunha. “The role of neutrophils in severe sepsis.” SHOCK. 2008. 30,1:3-9.

[4] K A Brown, S D Brain, J D Pearson, J D Edgeworth, S M Lewis, D F Treacher. “Neutrophils in development of multiple organ failure in sepsis.” Lancet. 2006. 368: 157-169.

[5] V. Y. Dombrovskiy, A. A. Martin, J. Sunderram, H. L. Paz. “Rapid increase in hospitalization and mortality rates for severe sepsis in the United States: A trend analysis from 1993 to 2003.” Critical Care Medicine. 2007;35, 5: 1244-1250.

[6] Angus DC, Linde-Zwirble WT, Lidicker J, et al: Epidemiology of severe sepsis in the United States: Analysis of incidence, outcome, and associated costs of care. Critical Care Medicine. 2001; 29:1303-1310.

[7] J. Xu, X.P. Gao, R. Ramchandran, Y.Y. Zhao, S.M. Vogel, A.B. Malik. Nonmuscle myosin light-chain kinase mediates neutrophil transmigration in sepsis-induced lung inflammation by activating B2 integrins. Nature Immunology. 2008; 9, 8. 880-886.

[8] B. McDonald, R. Urrutia, B.G. Yipp, C.N. Jenne, P. Kubes. Intravascular Neutrophil Extracellular Traps Capture Bacteria from the Bloodstream during Sepsis. Cell Host and Microbe. 2012;12. 324-333.

[9] J. Toyjanova, E. Bar-Kochba, C. Lopez-Fagundo, J. Reichner, D. Hoffman-Kim, C. Franck. High Resolution, Large Deformation 3D Traction Force Microscopy. PLOS.

04/2014;4. 1-12.

[10] Franck C, Hong S, Maskarinec SA, Tirrell DA, Ravichandran G (2007) Three-dimensional full-field measurements of large deformations in soft materials using confocal microscopy and digital volume correlation. Experimental Mechanics 47: 427-438.

[11] E. Bar-Kochba, J. Toyjanova, E. Andrews, K.-S. Kim, C. Franck. A Fast Iterative Digital Volume Correlation Algorithm for Large Deformations. Experimental Mechanics. 2015; 55: 261-274.

[12] Franck C, Maskarinec SA, Tirrell DA, Ravichandran G (2009) Quantifying cellular traction forces in three dimensions. Proceedings of the National Academy of Sciences of the United States of America 106: 22108-22113.

[13] Franck C, Maskarinec SA, Tirrell DA, Ravichandran G (2011) Three-Dimensional Traction Force Microscopy: A New Tool for Quantifying Cell-Matrix Interactions. Plos One 6: e17833.

[14] Long R, Hall MS, Wu M, Hui CY (2011) Effects of Gel Thickness on Microscopic Indentation Measurements of Gel Modulus. Biophysical journal 101: 643-650.

[15] S.R. Clark, M. Kelly, Z. Goodarzi, S. Chakrabarti (2007) Platelet TLR4 activates neutrophil extracellular traps to ensnare bacteria in septic blood. Nature Medicine 13: 463-469.

[16] K. Ley, C. Laudanna, M.I. Cybulsky, S. Nourshargh (2007) Getting to the site of inflammation: the leukocyte adhesion cascade updated. Nature Reviews 7: 678-689.

[17] M.R. Shalaby, B.B. Aggarwal, E. Rinderknecht, L.P. Svedersky, B.S. Finkle, M.A. Palladino, Jr (1985) Activation of human polymorphonuclear neutrophil functions by interferon-gamma and tumor necrosis factors. The Journal of Immunology 135: 2069-2073.

[18] R. Malhotra, R. Priest, M.I. Bird (1996) Role for L-selectin in lipopolysaccharide-induced activation of neutrophils. Journal of Biochemistry 320: 589-593.

[19] J. Toyjanova, et. al. "3D Viscoelastic Traction Force Microscopy." Royal Society of Chemistry, 2014. 10, 14: 8095-8106.

[20] Tse, Justin R., Engler, Adam J. "Preparation of Hydrogel Substrates with Tunable Mechanical Properties." Current Protocols in Cell Biology, 2010. doi:10.1002/0471143030.cb1016s4

[21] "EasySep Direct Human Neutrophil Isolation Kit." Stem Cell Technologies, www.stemcell.com/easysep-direct-human-neutrophil-isolation-kit.html.

Chapter 7

Appendix

Appendix A

Detailed Protocols

A.1 Glass coverslips surface modification

A.1.1 Hydrophobic coverslips

1) Prepare solution of 97% (v/v) hexane (Fisher Scientific, Waltham, MA), 2.5% (v/v) (tridecafluoro-1,1,2,2-tetrahydrooctyl)-triethoxysilane (SIT) (Gelest, Morrisville, PA), and 0.5% (v/v) acetic acid (Sigma-Aldrich, St. Louis, MO) in a glass Petri dish.

2) Place circular 25 mm glass coverslips into Petri dish and let swirl for 5 minutes.

3) Remove glass coverslips from solution and let dry at room temperature.

A.1.2 Hydrophilic coverslips

1) Rinse circular 25 mm glass coverslips in a Petri dish with ethanol for 5 minutes.

2) Prepare solution of 0.5% (v/v) 3-aminopropyltriethoxysilane (Sigma-Aldrich, St. Louis, MO) in ethanol.

3) Place circular 25 mm glass coverslips into Petri dish and let swirl for 5 minutes.

4) Rinse circular 25 mm glass coverslips in a clean Petri dish with ethanol.

5) Prepare solution of 0.5% glutaraldehyde (Polysciences, Inc., Warrington, PA) in deionized water.

6) Place circular 25 mm glass coverslips into Petri dish and let swirl for 30 minutes.

7) Rinse circular 25 mm glass coverslips in a Petri dish with deionized water.

8) Remove glass coverslips from Petri dish and place in single layer to dry in 30°C oven for 45 minutes.

A.2 Preparation of polyacrylamide hydrogels

1) Mix recommended volumes of DIH2O, acrylamide, bis, and beads together in 2 mL Eppendorf tube. Vortex for 30 seconds.

2) Split half of solution into second 2 mL Eppendorf tube (98.3 μL).

3) Take half of APS volume and TEMED volume (1.25 μL, 0.5 μL), and add to second Eppendorf tube. Vortex for 20-30 seconds. *Note: Polymerization reaction will begin once both APS and TEMED are added.*

4) Add 20 μL of gel solution to the middle of 25 mm circular hydrophilic glass coverslip, and cover with 25 mm circular hydrophobic glass coverslip. Ensure gel solution is evenly spread across glass coverslip.

5) Cover petri dish with foil and let sit for 20 minutes.

6) Add DIH2O to petri dish and let sit for 45 minutes.

7) Remove hydrophobic glass coverslips by gently using razor or Exact-O-Knife to split coverslips. Leave in PBS or DIH2O, or continue to gel surface functionalization.

A.3 Protein functionalization on polyacrylamide hydrogels

A.3.1 Polyacrylamide functionalization

1) Remove excess water from polyacrylamide gel with Kimwipe at 45° angle.

2) Make solution of 1 mg/mL sulfo-SANPAH in DIH2O. Will need 600 μL per coverslip (600 μg sulfo-SANPAH/coverslip).

3) Place gels in glass dish, and pipette 300 μL of sulfo-SANPAH solution onto each gel surface. Cover with foil and let stand for 10 minutes.

4) Transport to UV irradiation chamber with a wet Kimwipe. Irradiate for 15 minutes.

5) Remove darkened sulfo-SANPAH from gels by tilting dish and gently pipetting from edge of gel.

6) Add 300 μL sulfo-SANPAH onto each gel. Irradiate for 15 minutes.

7) Remove darkened sulfo-SANPAH.

8) Rinse 6 times for 5 minutes in PBS using shake table.

9) Remove excess PBS from polyacrylamide gel with Kimwipe at 45° angle. Continue to protein coating.

A.3.2 Protein coating

Prepare human fibronectin coating:

1) Dilute 1 mg/mL human fibronectin to 0.2 mg/mL solution using PBS. *Note: Do not re-freeze diluted solution. Only store human fibronectin at 1 mg/mL concentration.*

2) Cover polyacrylamide gel surface with 200 μL of 0.2 mg/mL fibronectin.

3) Add wet Kimwipe to dish, Parafilm plate, and leave overnight in 4°C fridge.

4) Remove from fridge and let warm to room temperature.

5) Rinse 2x with PBS.

6) Replace PBS with L-15 media + 2 mg/mL glucose before adding neutrophils.

Prepare human ICAM1 coating:

1) Dilute 0.1 mg/mL human ICAM1 to 50 μg/mL solution using 1.25% 10 mM HEPES and 48.75% 1x PBS. *Note: Do not re-freeze diluted solution. Only store human ICAM1 at 0.1 mg/mL concentration.*

2) Cover polyacrylamide gel surface with 200 μL of 50 μg/mL ICAM1.

3) Add wet Kimwipe to dish, Parafilm plate, and leave overnight in 4°C fridge.

4) Remove from fridge and let warm to room temperature.

5) Rinse 2x with PBS.

6) Replace PBS with L-15 media + 2 mg/mL glucose before adding neutrophils.

A.4 Human neutrophil isolation

A.4.1 EasySep protocol

1) Collect sample and add whole blood to 5 mL polystyrene round-bottom tube.

2) Vortex RapidSpheres for 30 seconds.

3) Add 50 μL/mL Isolation Cocktail to sample.

4) Add 50 μL/mL RapidSpheres to sample.

5) Mix and incubate at RT for 5 minutes.

6) Add 1X PBS to top up sample to 4 mL and mix.

7) Place tube into magnet and incubate at RT for 5 minutes.

8) Pick up magnet and pour enriched cell suspension into new 5 mL tube.

9) Add 50 μL/mL RapidSpheres to new tube and mix.

10) Place tube into magnet and incubate at RT for 5 minutes.

11) Pick up magnet and pour enriched cell suspension into new 5 mL tube.

12) Place tube into magnet and incubate at RT for 5 minutes.

13) Pipette out isolated neutrophils into new tube, and cells are ready to use.

A.4.2 Neutrophil cell membrane dye

1) Use AlexaFluor 488 actin cell membrane dye to fluorescently dye the isolated neutrophils.

2) Count isolated neutrophils in 1 mL PBS, and centrifuge into pellet (300 g, 4 min).

3) Add 100 μL Diluent C directly to cell pellet.

4) In separate 2 mL Eppendorf tube, make 100 μL solution of Diluent C and cell membrane dye. *Approximate ratio: 3 μL dye for 1 million human neutrophils*

5) Add 100 μL dye solution to cells, and let sit for 3 minutes.

6) Add 500 μL FBS to stop reaction, and fill Eppendorf tube with PBS.

7) Centrifuge into pellet, resuspend in 1 mL PBS, and re-count for accurate population number.